Supporting Information

Interfacial Engineering by Creating Cu-Based Ternary Heterostructures on C_3N_4 Tubes towards Enhanced Photocatalytic Oxidative Coupling of Benzylamines

Yunqi Fu,[a] Mang Zheng,[a] Qi Li,[a] Liping Zhang,[b,*] Shuai Wang,[c,*] V.V. Kondratiev [d], Baojiang Jiang[a,*]

[a] Key Laboratory of Functional Inorganic Material Chemistry, Ministry of Education of the People' s Republic of China, School of Chemistry and Materials Science, Heilongjiang University, Harbin 150080, China.

[b] Department of Chemistry and Biochemistry, Kent State University, Kent, OH 44242, USA

[c] Department of Food and Environment Engineering, Heilongjiang East University, Harbin, China

[d] Institute of Chemistry, Saint Petersburg State University, Russia.

E-mail: Lzhang30@kent.edu; 79652283@qq.com; jbj@hlju.edu.cn; jiangbaojiang88@sina.com

Table S1. Cu contents for different photocatalysts determined by inductively coupled plasma spectrometer (ICP).

Sample	**Cu content (%)**
$Cu/Cu_2O/Cu_3N/C_3N_4$-1	66.46
$Cu/Cu_2O/Cu_3N/C_3N_4$-2	60.48
$Cu/Cu_2O/Cu_3N/C_3N_4$-3	59.19
$Cu/Cu_2O/Cu_3N/C_3N_4$-4	33.47

Table S2. Elemental analysis results of different photocatalysts.

Sample	C (%)	N (%)	C/N
$Cu/Cu_2O/Cu_3N/C_3N_4$-1	5.32	8.63	0.6165
$Cu/Cu_2O/Cu_3N/C_3N_4$-2	6.52	10.90	0.5982
$Cu/Cu_2O/Cu_3N/C_3N_4$-3	11.8	20.46	0.5767
$Cu/Cu_2O/Cu_3N/C_3N_4$-4	9.10	15.07	0.6038

Table S3. Results of benzylamine oxidation coupling induced by $Cu/Cu_2O/Cu_3N/C_3N_4$-3 under different reaction conditions.

Condition	Conversion	Selectivity
Thermal (50℃)	33%	94%
Illumination	74%	98%
Photo-thermal	99%	98%

Table S4. Benzylamine oxidation coupling induced by $Cu/Cu_2O/Cu_3N/C_3N_4$-3 under different atmospheres.

Condition	Conversion	Selectivity
N_2	44%	98%
O_2	98%	95%
Air	99%	98%

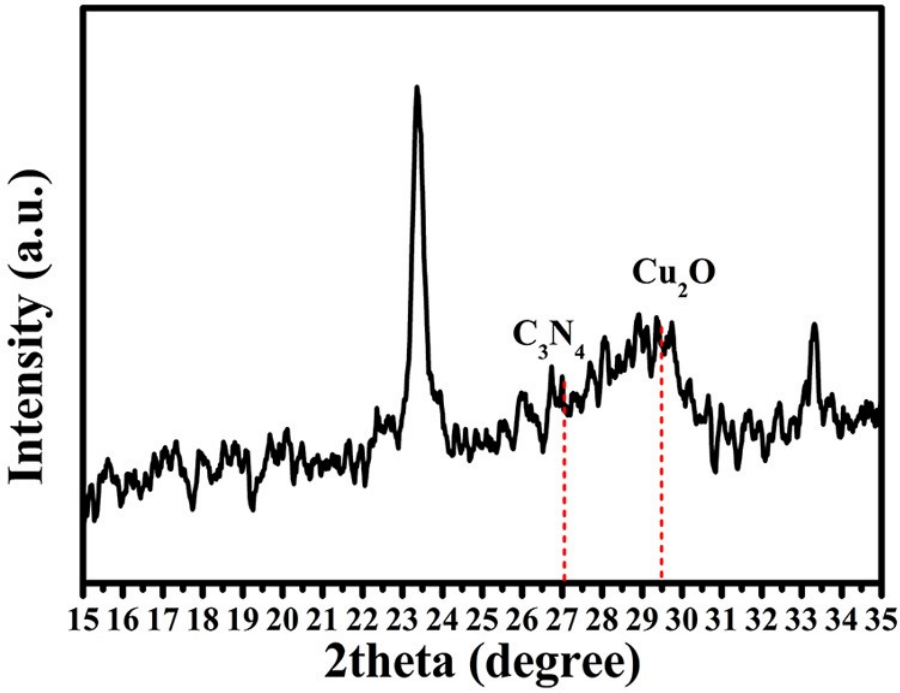

Figure S1. XRD partial enlarged view of $Cu/Cu_2O/Cu_3N/C_3N_4$-3.

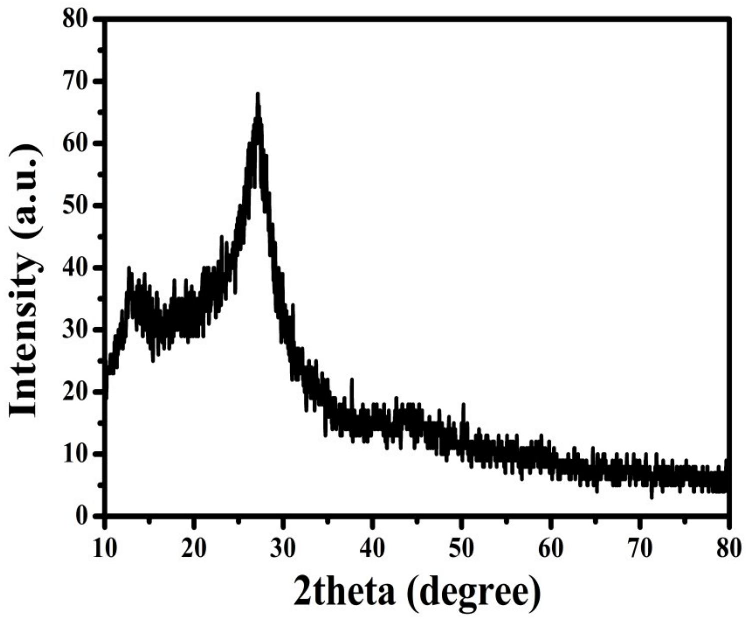

Figure S2. XRD pattern of the sample without adding copper acetate.

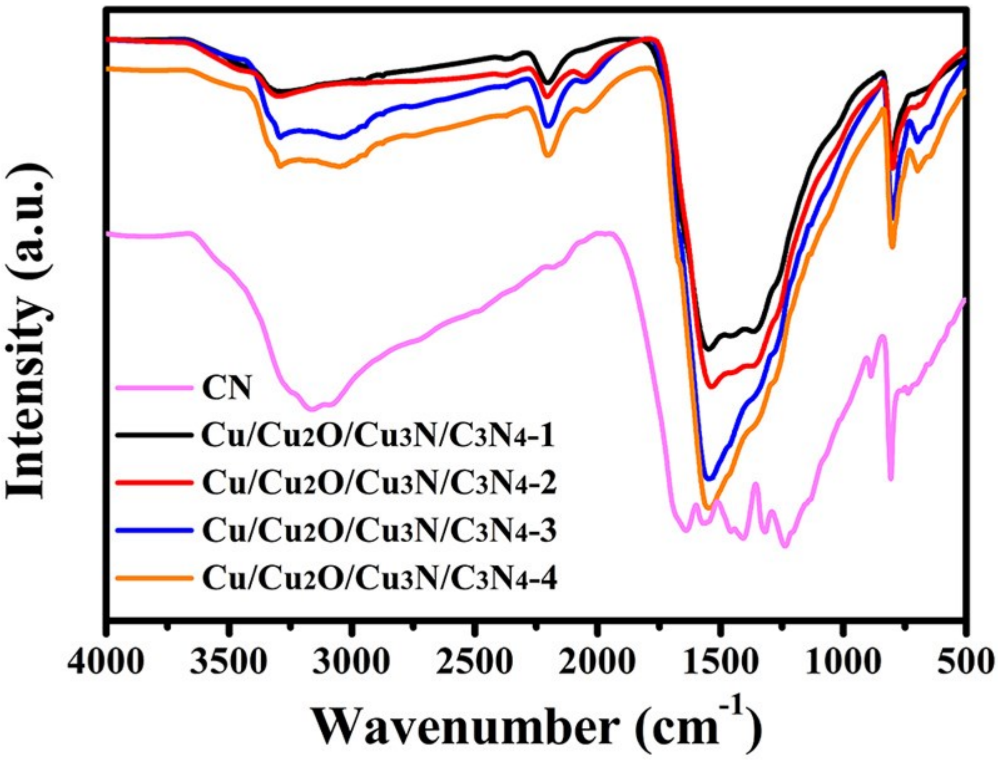

Figure S3. Fourier transform infrared spectrum of bulk carbon nitride and $Cu/Cu_2O/Cu_3N/C_3N_4$ of different molar ratio.

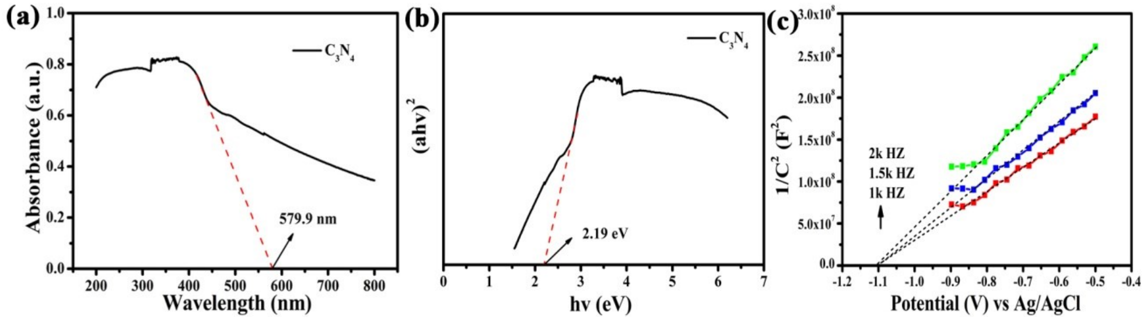

Figure S4. (a) Diffuse reflectance spectra (DRS) and (b) Tauc plots of C_3N_4. (c) Mott-Schottky plots of C_3N_4 at various frequencies (pH = 7).

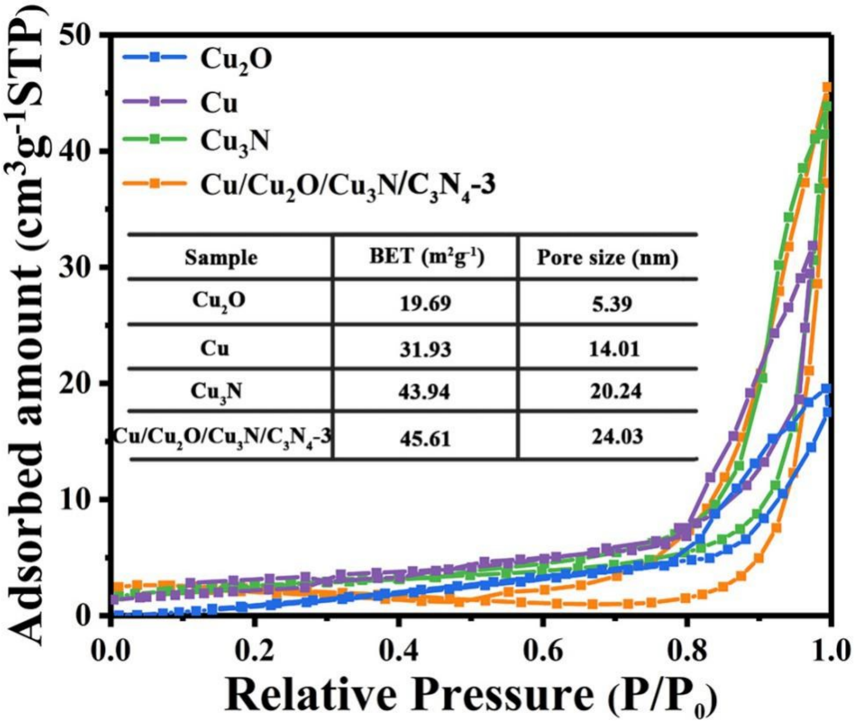

Figure S5. Nitrogen adsorption-desorption isotherms of Cu_2O, Cu, Cu_3N and $Cu/Cu_2O/Cu_3N/C_3N_4$-3. The inserted table shows the BET surface area and pore size.

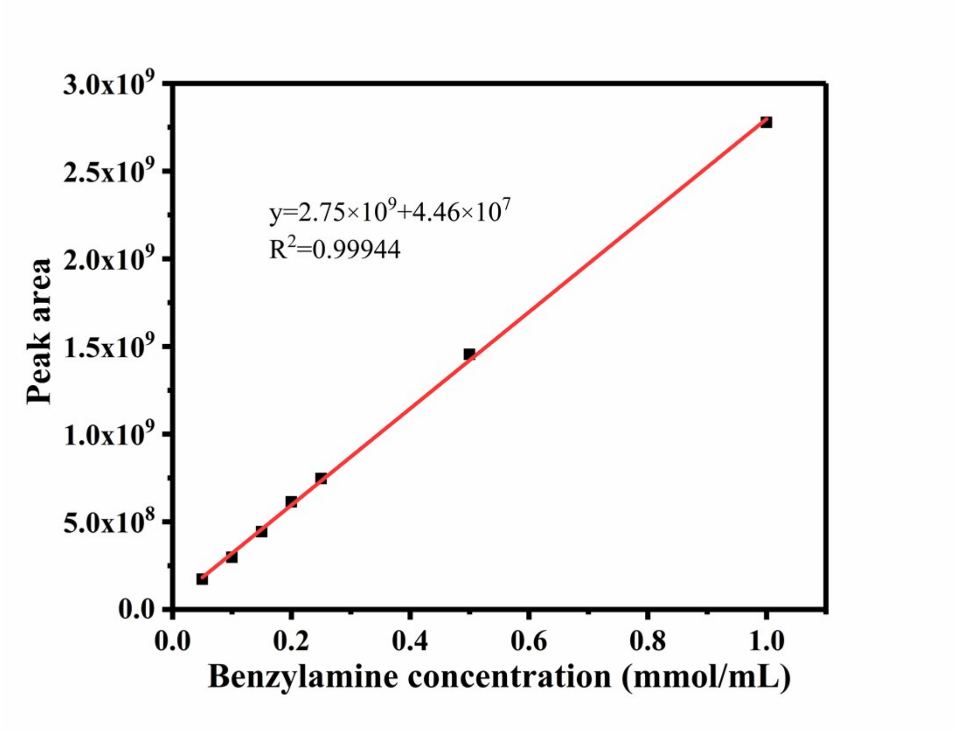

Figure S6. Standard calibration curve of benzylamine for gas chromatography.

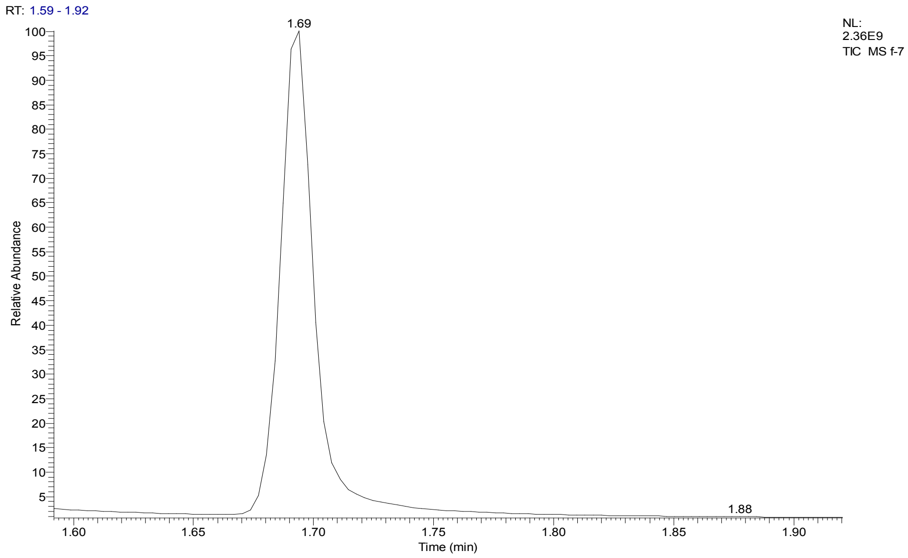

Figure S7. Chromatogram of chromatographic grade benzylamine.

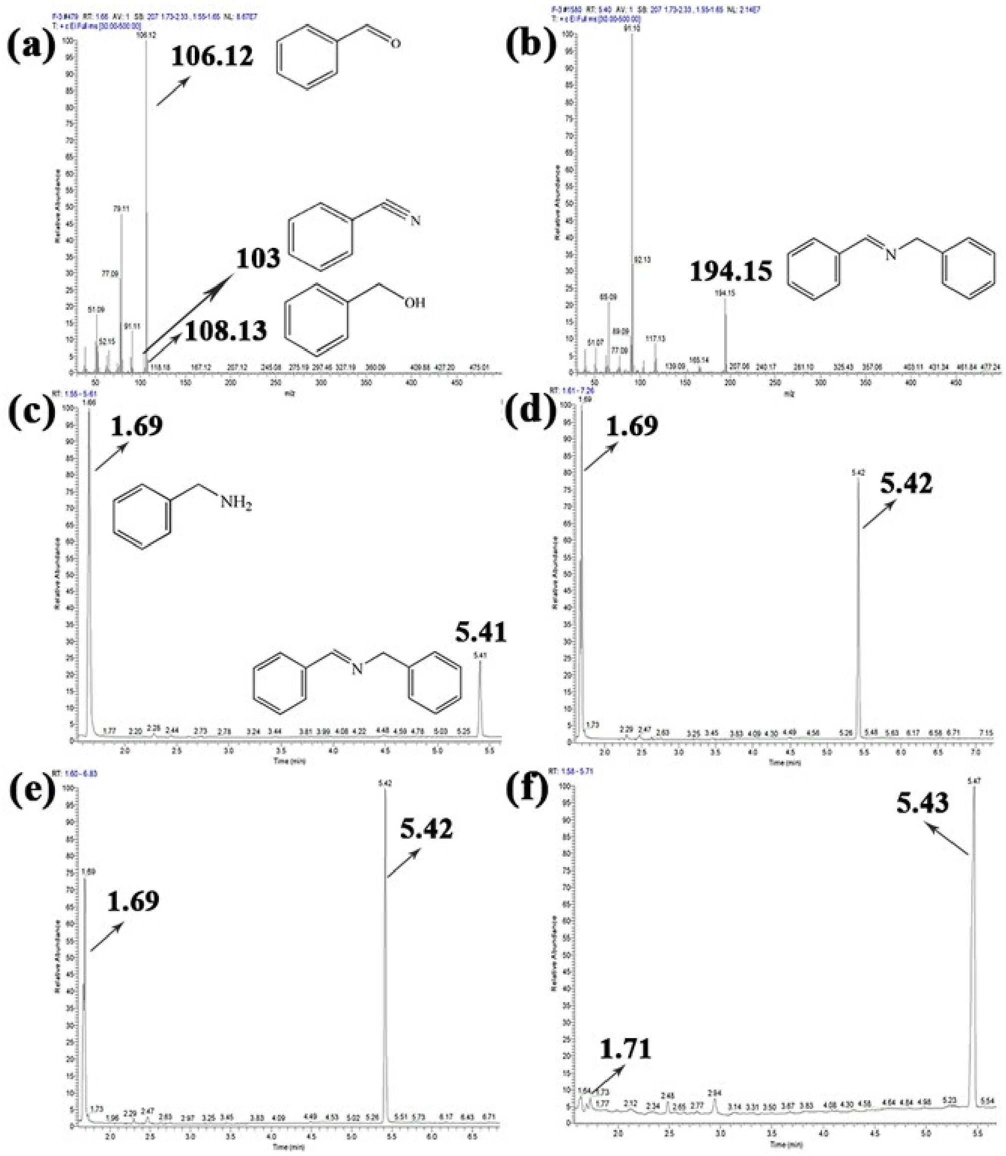

Figure S8. (a) Mass spectra of benzylamine and (b) imine at the 3rd hour of reaction. Chromatograms of the benzylamine coupling reaction at (c) 3rd hour, (d) 6th hour, (e) 9th hour and (f) 12th hour.